RESEARCH PAPER

Thermal and chemical durability of nitrogen-doped carbon nanotubes

Hao Liu · Yong Zhang · Ruying Li ·
Xueliang Sun · Hakima Abou-Rachid

Abstract Nitrogen-doped carbon nanotubes (CN_x tubes) with nitrogen content of 7.6 at.% are synthesized on carbon papers. Thermal and chemical stability of the nanotubes are investigated by thermogravimetric analysis, differential scanning calorimetry and X-ray photoelectron spectroscopy techniques. The results indicate that the nitrogen can be firmly kept in the nanotubes after annealing at 300 °C in air. Under an argon atmosphere, the nitrogen would not release until 670 °C, and half of the nitrogen incorporated is released after annealing at 700 °C for 30 min. Chemical stability investigation indicates that the nitrogen incorporated in the nanotubes is very stable under the thermal and acid environment comparable to working condition of proton exchange membrane (PEM) fuel cells. Profile of the nitrogen species inside the nanotubes reveals that graphite-like nitrogen releases slower than any other kind of nitrogen in the nanotubes during the chemical stability measurement. These CN_x tubes synthesized by this simple chemical vapor deposition method are expected to be suitable for many applications, such as PEM fuel cells that work under both thermal and corrosive conditions and some other mild thermal environments.

Introduction

Nitrogen-doped carbon nanotubes (CN_x tubes) have attracted particular research interest because of their applications in producing different types of nanodevices with tuning properties such as nanoscale electronics (Huang et al. 2002), biosensors (Huang et al. 2002), nanoenergetic materials (Rossi et al. 2007) and fuel cells (Subramanian et al. 2009). Previous reports have indicated that controlled nitrogen doping can modulate the morphology, improve the reactivity and enhance the field emission of the pristine carbon nanotubes. Doped nitrogen atoms mainly exist in two forms, substitutional and pyridinic nitrogen (also called graphite-like and pyridine-like nitrogen), both are chemically active for improving the surface reactivity of CNTs because of the presence of electron donor (Nevcidomskyy et al. 2003). Furthermore, their physical and electrical properties are also altered because of the change of local electron density in

H. Liu · Y. Zhang · R. Li · X. Sun (✉)
Department of Mechanical and Materials Engineering,
University of Western Ontario, London,
ON N6A 5B9, Canada
e-mail: xsun@eng.uwo.ca

H. Abou-Rachid
Defense Research & Development Canada,
Valcartier, 2459 Boulevard PieXI nord, Québec,
QC G3J 1X5, Canada

materials by introducing nitrogen atoms (Miyamoto et al. 1997). Obviously, it is prerequisite to maintain the stable nitrogen content and profile within the nanotubes to sustain their performance durability of CN_x tubes.

However, some of the nitrogen species are subject to loss from CNTs. It has been reported that nitrogen will release to some extent when CN_x tubes are exposed to air (Tang et al. 2004). Investigation of thermal properties is also important in understanding the structure of the CN_x tubes as well as in their applications. Thermogravimetric analysis (TGA) has been widely used to investigate the thermal stability of the CN_x tubes as well as the distribution and species of the carbon phases present in CN_x tubes either in air (Tao et al. 2007; Maldonado and Stevenson 2005) or in a protective gas flux (Zhao et al. 2005). In the application fields, the stability of different nitrogen species incorporated in CN_x tubes under a general condition is needed. When CNTs are used in fuel cells as catalyst supporting materials (Villers et al. 2006), the tubes are working in an acidic atmosphere. When CNTs are used in electronic systems, they might be machined at a thermal environment and heat would also be generated because of the Joule effect. Therefore, it is of importance to investigate the durability of nitrogen inside the CN_x tubes to make sure they can meet the requirements of device manipulation and practical working conditions. However, to our knowledge, the release of nitrogen from carbon nanotubes is only studied in an extreme condition, a vacuum of $<10^{-8}$ Torr (Choi et al. 2005). Thermal and chemical durability of the nitrogen species incorporated in CN_x tubes is seldom discussed.

Among different substrates, silicon (electrical semiconducting) and carbon microfibers (electrical conductive) are two representatives. The aligned growth of CNTs on silicon substrate provides the possibility of integrating CNTs directly into silicon technology. Meanwhile, because carbon paper is electrically conducting and the CNTs on carbon paper adhere firmly to the substrate leading to electrical contact, much high-density CNTs on commercially used carbon paper substrate can be used as Pt support electrodes for fuel cell applications (Villers et al. 2006; Sun et al. 2003). However, it is a challenge to deposit catalytic nanoparticles on carbon fiber surface because of its hydrophobic nature. Therefore, other methods such as silane-assisted catalytic nanoparticles

deposition method had to be used to obtain high-density CNTs on carbon paper (Sun et al. 2003; Sun et al. 2007).

In this article, CN_x tubes are grown on carbon paper with the help of a thin aluminum film as buffer layer via a simple floating catalyst chemical vapor deposition (FCCVD). The post-annealing effects on CN_x tubes are studied. The thermal and chemical stability of CN_x tubes and different nitrogen species incorporated in CN_x tubes are studied by means of TGA, differential scanning calorimetry (DSC) and X-ray photoelectron spectroscopy (XPS) techniques.

Experimental section

Before CN_x tubes were grown, the carbon paper was sputtered with a thin aluminum buffer layer (thickness 30 nm) to prepare the substrate surface to obtain uniform and high-density CN_x tubes. The sputtering was carried out under a pressure of 4.0 mTorr and at a power of 300 W.

The synthesis of CN_x tubes was carried out by a FCCVD system under an argon/ethylene flow with ferrocene as the catalyst precursor and melamine as the nitrogen source that has been reported elsewhere (Liu et al. 2010). Briefly, substrates were located in the center of the reaction chamber while melamine and ferrocene were placed at the entrance of the furnace. When the chamber was heated to 950 °C, the two layer mixture reached 350 °C, which is more than the sublimation temperatures of ferrocene and melamine. At the same time, ethylene was introduced into the system. Thus, the ferrocene and melamine were brought into the high-temperature region where the pyrolysis and synthesis occurred at 950 °C. After 15 min, the ethylene gas was turned off and the system cooled down to room temperature in the flowing Ar gas.

TGA and DSC were performed to the as-grown CN_x tubes at a heating rate of 15 °C/min under either static air condition or protective gas flux. Then, CN_x tubes were heated at selected temperatures for 30 min in air or protective gas flux. Besides this annealing treatment, the as-grown CN_x tubes were also treated by an acid process. The as-grown CN_x tubes were suspended in a mixture of 1-M HCl and 1-M HNO_3 and stirred at 80 °C to simulate the working environment in PEM fuel cells and other potential

applications. After this acid treatment, the CN_x tubes were washed with distilled water and filtered for three times and then dried in vacuum oven at a temperature of 50 °C.

The morphology of as-grown and annealed CN_x tubes was examined by Hitachi S-4800 field-emission scanning electron microscopy (SEM) operated at 5.0 kV, Philips CM10 transmission electron microscopy (TEM) operated at 80 kV. The nitrogen content and the stability of the nitrogen incorporated in CN_x tubes were studied by Kratos Axis Ultra Al (alpha) X-ray photoelectron spectroscopy (XPS) operated at 14 kV.

Result and discussion

Figure 1 shows typical SEM and TEM images of the as-synthesized CN_x tubes. The substrate is covered by CN_x tubes in the form of bundles. The length of each bundle is about 60 μm. Comparing with non-doped CNTs we reported earlier (Liu et al. 2008), CN_x tubes has a faster growth rate and the tubes tend to be curved. TEM image shows that all nanotubes exhibit an irregular and inter-linked corrugated morphology. The outer diameter reaches as large as 100–120 nm which is bigger than that of non-doped CNTs. Meanwhile, the inner diameters of CN_x tubes also increase compared with their non-doped counterpart. However, the wall thickness of nanotubes decreases with increasing nitrogen content. The nanotubes are curved, as observed from SEM, because of imperfect interlinks of the bamboo-like compartment. The nanotube morphology strongly depends on the nitrogen content, which is identified by HRTEM and Raman spectroscopy and reported with earlier report (Liu et al. 2010). The results show that the degree of long-range ordered crystalline perfection of CN_x tubes decreases and more defects and disorders are introduced with the incorporation of nitrogen.

TGA was conducted to assess thermal stabilities of the CN_x tubes under both air and protective atmosphere (nitrogen in this case). The TGA curves are given in Fig. 2. Figure 2a shows the TGA curve performed in air. A unique inflexion appears at 530 °C and then the weight of CN_x tubes losses drastically because of the combustion of carbon in air atmosphere. The residual bulk mass percentage after oxidation was 2 %. It has been reported that

the oxidative temperature of non-doped carbon nanotubes is around 600–750 °C (Tao et al. 2007; Huang et al. 2003). Our DSC shows a broad oxidation peak in the range of 530–730 °C, which is lower than the oxidative temperature for pure non-doped CNTs. The observed lower thermal decomposition temperature suggests that the CN_x tubes are much easier to be oxidized than non-doped CNTs due the existence of more disorders and considerably more edge plane sites (Liu et al. 2010; Tao et al. 2007; Maldonado et al. 2006). Comparing with the sample oxidized in air atmosphere, the thermal stability of the CN_x tubes under nitrogen atmosphere is displayed in Fig 2b. The inflexion present at 670 °C, before which only 1 % weight was lost which is attributed to contaminated water vapor. The weight loss increases at elevated temperature. This will be discussed later.

Figure 3 shows TEM images of the CN_x tubes after (a) 700 °C annealing and (b) acid treatment. Compared with the TEM images in Fig. 1, all tubes demonstrate a corrugated structure. The morphology and structure scarcely change after annealing or acid treatment, although the nitrogen content changes to some extent.

To obtain more information on the relationship of nitrogen concentration in the CN_x tubes and different treatment conditions, XPS analysis was carried out after selected post-treatment processes at 300 and 700 °C under air or protective gas flux. The full-range XPS spectra of CN_x tubes are exhibited in Fig. 4a. We obtained three main peaks at 285, 401 and 531 eV. They are attributed to C 1 s, N 1 s and O 1 s signal, respectively. The strong C peak can be assigned to sp^2-hybridized carbon, which is the major component in CN_x tubes. The N peak will be discussed in detail later. The N concentration contained in the nanotubes, defined as N/C at.%, is estimated by the area ratio of the nitrogen and carbon peaks (Liu et al. 2010; Nath et al. 2000). The nitrogen content of each sample has been calculated and listed in Table 1. It demonstrates that the nitrogen content hardly changed after treated at a temperature lower than 300 °C. When the annealing temperature raised to 700 °C, the nitrogen content dropped to 3.2 %.

The N 1 s signals of these samples are shown in Fig. 4b–e. The symmetric N 1 s spectra indicate the existence of several components. The spectra are fitted into four to five peaks. The peaks around 399.0–400.1 eV and
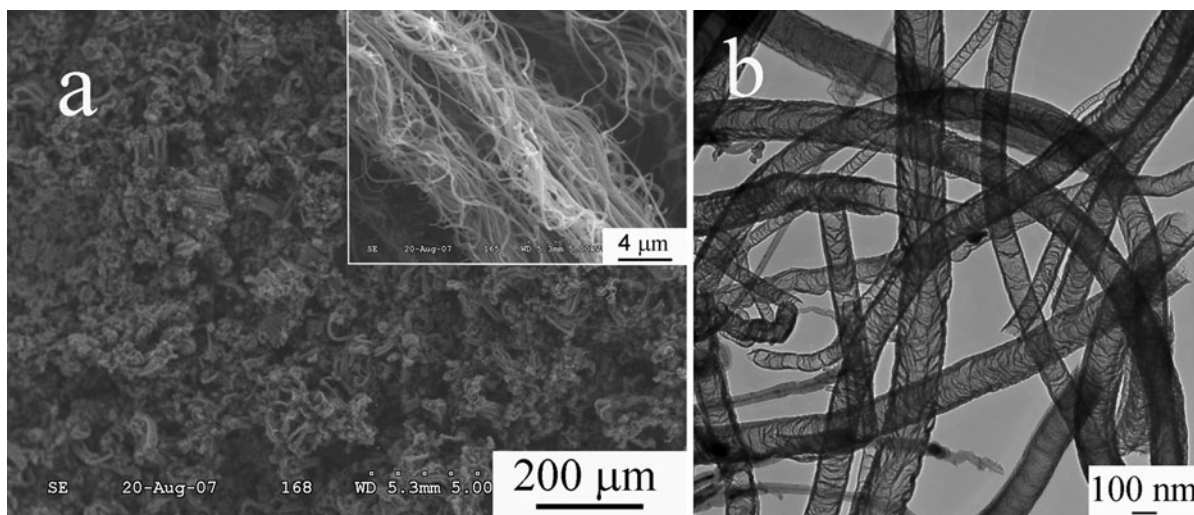
Fig. 1 SEM and TEM images of the CN_x tubes synthesized on carbon paper
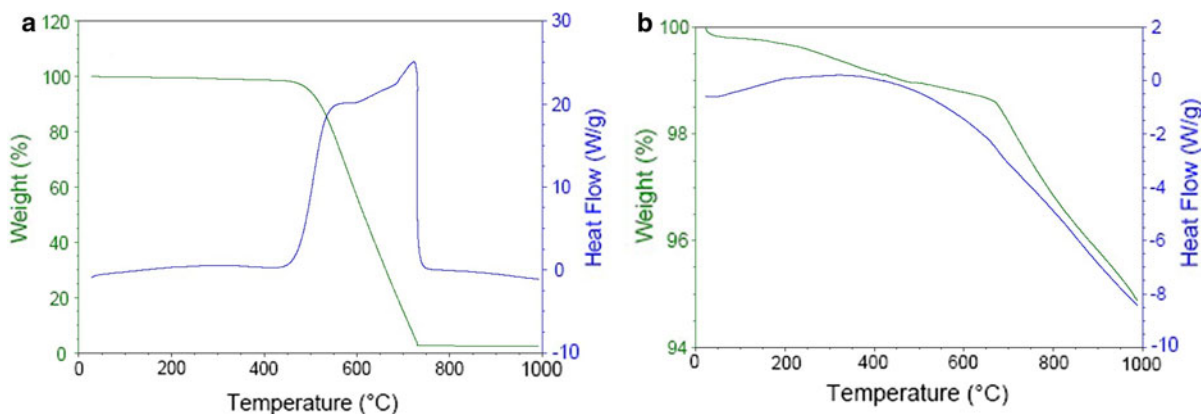

Fig. 2 TGA and DSC curves of the CN_x tubes under **a** air and **b** nitrogen atmosphere

401.5–402.4 eV are attributed to pyridine-like nitrogen and graphite-like nitrogen (Liu et al. 2010). Pyridine-like atoms contribute to the π system with a pair of π electrons and bonding to two carbon atoms. While the graphite-like nitrogen corresponds to highly coordinated nitrogen atoms substituting inner carbon atoms on the graphite layers. The peaks around 403.1–403.8 eV are assigned to oxidized nitrogen which are bonded with oxygen (Liu et al. 2010). The peaks around 405.3–406.1 eV are ascribed to the nitrogen atoms that form endohedral or exohedral complex with carbon–carbon bond on the tube walls (Liu et al. 2010), which are called sorbed nitrogen. It has also been proved that these nitrogen atoms are covalently bound to the carbon nanotubes (Zhao et al. 2002). The highest bonding energy band arise at around

407.8–408.9 eV can be attributed to molecular nitrogen because previous reports show molecular nitrogen can be encapsulated inside the tubes (Reyes-Reyes et al. 2004) or exist as intercalated form between graphite layers during the formation of CN_x tubes (Choi et al. 2004).

The nitrogen profiles are listed in Table 1 as well. The profiles of the samples annealed at a temperature <300 °C did not show big differences. But after the annealing at 700 °C, molecular nitrogen peak was not observed in this sample. This phenomenon implies that molecular nitrogen is weakly bonded to the graphite layers and first released during the annealing process. Another noticeable phenomenon is that the nitrogen content of the sample falls to 3.2 % from the original 7.6 %, and both pyridine-like nitrogen and
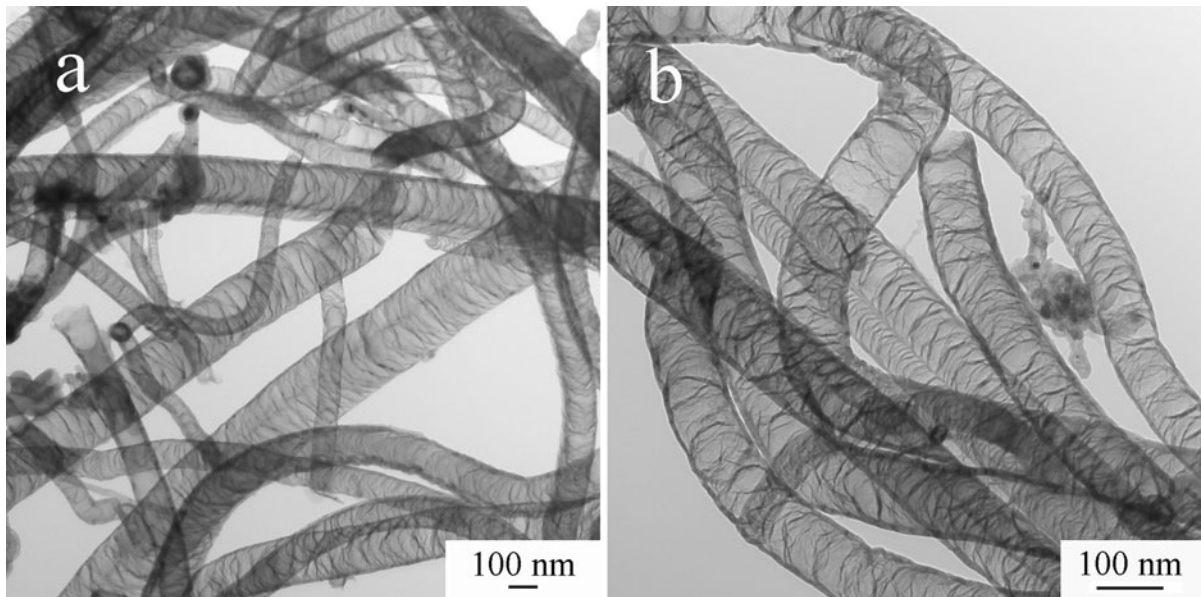
Fig. 3 TEM images of the CN_x tubes treated **a** at 700 °C and **b** in acid

graphite-like nitrogen decreases after annealed at 700 °C, which may be because of the partial burn-off of the nanotubes during the high-temperature annealing. In addition, the peak of pyridinic nitrogen shifts from 399.0 eV to 400.1 eV, which can be attributed to pyridinic nitrogen in association with oxygen functionality (Kapteijn et al. 1999).

Thirdly, after annealing at 700 °C, the relative intensity of pyridine-like nitrogen to graphite-like nitrogen decreases visibly. This implies that the removal of pyridine-like nitrogen is quicker than that of graphite-like nitrogen, although both of them are releasing from CN_x tubes at high temperature. Because the graphite-like nitrogen has a higher energy than the pyridine-like nitrogen (Chen et al. 2006; Wang 2006), it is logical to observe that pyridine-like nitrogen releases quicker than graphite-like nitrogen. The fourth perceptible fact is that the ratio of N-oxidic (NO_x) species becomes more intense after annealing at 700 °C. Although no precursors containing oxygen were used in the experiment, the exposure of the samples to air may involve oxygen contaminants and aluminum oxide can be formed during the growth of the nanotubes because of the aluminum buffer layer on the substrate (Liu et al. 2008). NO_x species were possibly formed by the reaction of N atoms with oxygen contaminants or oxide substrates at the

elevated temperature. This is in consistent with the XPS survey spectra of the sample as shown in Fig. 4a, in which oxygen amount reaches its maximum after the sample was annealed at 700 °C. Now the weight loss of CN_x tubes after 670 °C under a nitrogen atmosphere can be assigned to the partial burn-off of the CN_x tubes and loss of nitrogen species incorporated in CN_x tubes.

The nitrogen species stability in an acid environment is also studied. In this treatment, residue catalyst should also be removed if they are exposed to environment. However, in our calculation, only nitrogen and carbon are taken into consideration; thus, removal of the catalyst will have no effect in the final results. The XPS full scan was shown in Fig. 4a, and the N 1 s spectrum and related nitrogen profile are demonstrated in Fig. 4f and Table 1, separately. The nitrogen content slightly increases after acid treatment. That is because that the carbon impurities such as graphite nanoparticles and amorphous carbons can be eliminated after washing with acid (Kwon and Kim 2005). The molecular nitrogen released after acid treatment because of its weak bonding to graphite layers. The intensity of graphite-like nitrogen increases because graphite-like nitrogen has a higher bonding energy and graphite-like nitrogen atoms are located in inner graphene layers
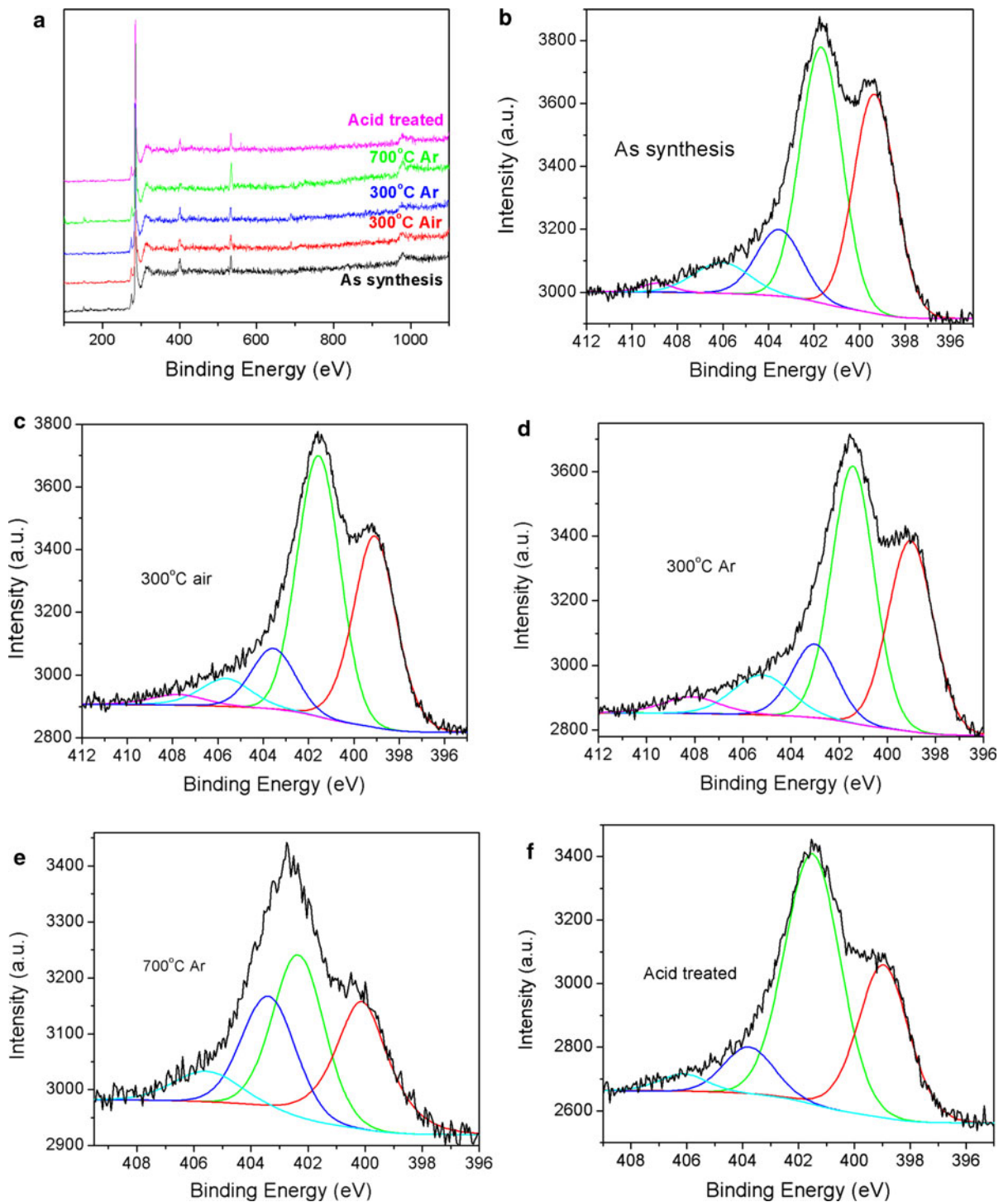
Fig. 4 XPS spectrum of the CN_x tubes treated at different conditions including different temperature and acid treatment **a** in full range and N 1 s XPS spectrum of the CN_x tubes **b** as synthesized, treated at **c** 300 °C in air, **d** 300 °C in argon, **e** 700 °C in argon and **f** at 80 °C in acid

Table 1 Nitrogen content and related detailed nitrogen distribution of CN_x tubes treated in different conditions

Treating conditions	Nitrogen content (%)	Pyridine-like nitrogen (%)	Graphite-like nitrogen (%)	NO_x (%)	Sorbed nitrogen (%)	Molecular nitrogen (%)
Non-doped counterpart	0	0	0	0	0	0
As synthesis	7.6	35.1	42.7	14.1	6.9	1.2
300 °C air	7.5	31.7	46.5	12.8	6.3	2.7
300 °C argon	7.4	31.2	42.2	13.4	9.5	3.7
700 °C argon	3.2	26.8	36.2	26	11.0	–
Acid treated	8.9	28.3	56.6	11.3	3.7	–

which is hard for acid to achieve. On the other hand, pyridine-like nitrogen prefers to exist at the open edges of the bamboo kink to stop their growth (Wang 2006), then it is easier for acid to react with pyridine-like nitrogen atoms.

Conclusions

High yield CN_x tubes are synthesized on carbon paper substrate. The nitrogen incorporated in CN_x tubes is very stable at a temperature lower than 300 °C or in an acid environment, which means the CN_x tubes synthesized by this simple FCCVD are suitable to be used in the applications in which the working condition is not very rigorous. The nitrogen starts to release at 670 °C. After a 30-min treatment at 700 °C under a protective atmosphere, half of the nitrogen remains in CN_x tubes. We also notice that the loss of graphite-like nitrogen is slower than any other kinds of nitrogen which means that the graphite-like nitrogen is most stable among all five kinds of nitrogen species. These CN_x tubes synthesized by this simple CVD method are expected to be suitable for many applications such as PEM fuel cells that work under both thermal and corrosive conditions and some other mild thermal environments.

References

Chen H, Yang Y, Hu Z, Huo K, Ma Y, Chen Y et al (2006) Synergism of C_5N six-membered ring and vapor–liquid–solid growth of CN_x nanotubes with pyridine precursor. J Phys Chem B 110(3):16422–16427

Choi HC, Baes SY, Park J, Seo K, Kim C, Kim B et al (2004) Experimental and theoretical studies on the structure of N-doped carbon nanotubes: possibility of intercalated molecular N_2. Appl Phys Lett 85(23):5742–5744

Choi HC, Bae SY, Jang WS, Park J, Song HJ, Shin HJ et al (2005) Release of N_2 from the carbon nanotubes via high-temperature annealing. J Phys Chem B 109:1683–1688

Huang W, Taylor S, Fu K, Lin Y, Zhang D, Hanks TW et al (2002) Attaching proteins to carbon nanotubes via dimide-activated amidation. Nano Lett 2(4):311–314

Huang W, Wang Y, Luo G, Wei F (2003) 99.9 % purity multi-walled carbon nanotubes by vacuum high-temperature annealing. Carbon 41(13):2585–2590

Kapteijn F, Moulijn JA, Matzner S, Boehm HP (1999) The development of nitrogen functionality in model chars during gasification in CO_2 and O_2. Carbon 37(7):1143–1150

Kwon JY, Kim HD (2005) Preparation and properties of acid-treated multiwalled carbon nanotube/waterborne polyurethane nanocomposites. J Appl Polym Sci 96:595–604

Liu H, Zhang Y, Arato D, Li R, Mérel P, Sun X (2008) Aligned multi-walled carbon nanotubes on different substrates by floating catalyst chemical vapor deposition: critical effects of buffer layer. Surf Coat Tech 202:4114–4120

Liu H, Zhang Y, Li R, Sun X, Désilets S, Abou-Rachid H et al (2010) Structural and morphological control, nitrogen incorporation and stability of aligned nitrogen-doped carbon nanotubes. Carbon 48:1498–1507

Maldonado S, Stevenson KJ (2005) Influence of nitrogen doping on oxygen reduction electrocatalysis at carbon nanofiber electrodes. J Phys Chem B 109:4707–4716

Maldonado S, Morin S, Stevenson KJ (2006) Structure, composition, and chemical reactivity of carbon nanotubes by selective nitrogen doping. Carbon 44(8):1429–1437

Miyamoto Y, Cohen ML, Louie SG (1997) Theoretical investigation of graphitic carbon nitride and possible tubule forms. Solid State Commun 102(8):605–608

Nath M, Satishikumar BC, Gobindaraj A, Vinod CP, Rao CNR (2000) Production of bundles of aligned carbon and

carbon–nitrogen nanotubes by the pyrolysis of precursors on silica-supported iron and cobalt catalysts. Chem Phys Lett 322(5):333–340

Nevcidomskyy AH, Csanyi G, Payne C (2003) Chemically active substitutional nitrogen impurity in carbon nanotubes. Phys Rev Lett 91(10):105502

Reyes-Reyes M, Grobert N, Kamalakaran R, Seeger T, Golberg E, Ruhle M et al (2004) Efficient encapsulation of gaseous nitrogen inside carbon nanotubes with bamboo-like structure using aerosol thermolysis. Chem Phys Lett 396:167–173

Rossi C, Zhang K, Esteve D, Alphose P, Tailhades P, Vahlas C (2007) Nanoenergetic materials for MEMS: a review. J Microelectromech Syst 16(4):919–931

Subramanian NP, Li X, Nallathambi V, Kumaraguru SP, Colon-Mercado H, Wu G et al (2009) Nitrogen-modified carbon-based catalysts for oxygen reduction reaction polymer electrolyte membrane fuel cells. J Power Sources 188(1):38–44

Sun X, Li R, Villers D, Dodelet JP, Desilets S (2003) Composite electrodes made of Pt nanoparticles deposited on carbon nanotubes grown on fuel cell backings. Chem Phys Lett 379(1–2):99–104

Sun X, Li R, Stansfield B, Dodelet JP, Menard G, Desilets S (2007) Controlled synthesis of pointed carbon nanotubes. Carbon 45(4):732–737

Tang C, Bando Y, Golberg D, Xu F (2004) Structure and nitrogen incorporation of carbon nanotubes synthesized by catalytic pyrolysis of dimethylformamide. Carbon 42(12–13): 2625–2633

Tao XY, Zhang XB, Sun FY, Cheng JP, Liu F, Luo ZQ (2007) Large-scale CVD synthesis of nitrogen-doped multi-walled carbon nanotubes with controllable nitrogen content on a $Co_xMg_{1-x}MoO_4$ catalyst. Diamond Relat Mater 16(3): 425–430

Villers D, Sun SH, Serventi AM, Dodelet JP, Desilets S (2006) Characterization of Pt nanoparticles deposited onto carbon nanotubes grown on carbon paper and evaluation of this electrode for the reduction of oxygen. J Phys Chem B 110(51):25916–25925

Wang EG (2006) Nitrogen-induced carbon nanobells and their properties. J Mater Res 21(11):2767–2773

Zhao M, Xia Y, Ma Y, Ying M, Liu X, Mei L (2002) Exohedral and endohedral adsorption of nitrogen on the sidewall of single-walled carbon nanotubes. Phys Rev B 66:155403

Zhao YC, Lu DL, Zhou HW, Tian YJ (2005) Turbostratic carbon nitride prepared by pyrolysis of melamine. J Mater Sci 40:2645–2647